

"Local Density Approximations in Quantum Chemistry
and Solid State Physics"

Editors: Jens Peder Dahl and John Avery

Plenum Press, New York and London, 713-732, 1984.

MULTIPOLE EXPANSION AS AN ALTERNATIVE

REPRESENTATION OF CHARGE DENSITY

Kaarle Kurki-Suonio and Riitta Salke

University of Helsinki
Department of Physics
Siltavuorenpenger 20 D
SF-00170 Helsinki 17
Finland

1. INTRODUCTION

In charge density studies the problems of analysis cannot be separated from problems of representation. The aim of the analysis is to obtain chemically and physically meaningful information on the structure, bonding and dynamics of the atoms in a crystal. But in order to detect this kind of information from the charge density we need a clear enough picture of the three-dimensional charge distribution function represented by the diffraction data or by the model fitted to the data. Problems of visualization of the information may seem physically trivial, but in practice they have proved to be essential. The article by Smith, Price and Absar¹ demonstrates these difficulties very clearly while showing different ways by which one has tried to overcome them.

In principle the problem is just the illustration of a real function in three-dimensional space, for which we should need four dimensions. In the study itself one can resort to three-dimensional models and for demonstration purposes time may be useful as the third dimension. However, the journals still are the main forum of scientific communication, which forces us to restrict into two-dimensional illustrations.

Smith et al.¹ demonstrate beautifully, how one can make use of modern computer techniques to produce different kinds of perspective views and projections to visualize e.g. the development of the shape of a molecule, when looked on different charge density values. Still, simple two-dimensional contour maps are the most common means

of representation and often the only one which can be used when computing and plotting facilities are restricted.

The multipole expansion offers another completely different possibility of representation. At present multipole expansions are used in many different, often quite sophisticated ways for analysis of diffraction data. However, when first introduced by Atoji² the main implication was just their use for representation of the charge density. This original purpose has largely been neglected in spite of its several obvious advantages.

In this article we discuss the representational possibilities offered by multipole expansions as an alternative to more conventional map representations and demonstrate, how they can be used to obtain quantitative information on significant features of the charge density distribution.

2. THE MULTIPOLE EXPANSION

By multipole expansion of the charge density we mean an expansion of the form

$$\rho(\bar{\mathbf{r}}) = \sum_{\ell mp} \frac{1}{N_{\ell mp}} \rho_{\ell mp}(r) y_{\ell mp}(\theta, \phi) \quad (1)$$

cf. Kurki-Suonio.³ It is an expansion of $\rho(\mathbf{r})$ around a given origin in terms of conventional spherical co-ordinates r, θ, ϕ using real spherical harmonics

$$y_{\ell m \pm} \sim P_{\ell}^m(\cos\theta) \begin{matrix} \cos m\phi \\ \sin m\phi \end{matrix}, \quad \ell = 0, 1, \dots, \quad m = 0, 1, \dots, \ell$$

with the normalization $\int (y_{\ell mp})^2 d\Omega = N_{\ell mp}^2$. We shall refer to ℓ as the order of the term.

The spherical harmonics are well-known standard functions. So, the illustration of the behaviour of each term requires only representation of the radial density $\rho_{\ell mp}(r)$ as a function of the distance r from the origin. Given the function $\rho(\mathbf{r})$ and the origin, the expansion (1) is unique. Thus, we have a representation of the three-dimensional charge density in terms of a set of one-dimensional functions. This yields a quantitative illustration of the charge density around the origin in all directions simultaneously in terms of a set of curves $\rho_{\ell mp}(r)$.

The perspicuity of this representation decreases rapidly with increasing number of terms required. However, taking the origin at the site of the atomic center few low-order terms are necessary to

represent the charge density of the atom and its close surroundings. Moreover, the harmonics can be site-symmetrized i.e. adapted to the point symmetry of the atomic site, which effectively minimizes the number of terms.^{3,4}

For the crystal charge density the radial densities around any fixed point \mathbf{r}_0 can be expressed in terms of the crystal structure amplitudes in the form

$$\rho_{\ell mp}(\mathbf{r}) = \frac{4\pi(-i)^\ell}{VN_{\ell mp}} \sum_{\bar{\mathbf{H}}} F_{\bar{\mathbf{H}}} \exp(-2\pi i \bar{\mathbf{H}} \cdot \bar{\mathbf{r}}_0) j_\ell(2\pi \bar{\mathbf{H}} r) y_{\ell mp}(\theta_{\bar{\mathbf{H}}}, \phi_{\bar{\mathbf{H}}}) \quad (2)$$

Taking \mathbf{r}_0 to be the position of each atom of the asymmetric unit in succession we effectively get representations of the atomic charge densities when the radial densities are looked only at small enough distances r . Conventional multipole models used in charge density studies involve a division of the crystal charge density into its atomic constituents; each is assumed to take the form of a multipole expansion. This division and hence the expansions are not unique but depend on the assumed motions of the atoms and on the analytical form chosen for the radial densities. Such use of the multipole expansions always involves some sophisticated interpretation of the charge density. Eq. (2) does not yield any such division. It just gives a pure representation of the crystal charge density as an alternative to contour maps, but is concentrated to the region of each atom separately.

The nature of the representation obtained in this way is certainly very much different in nature from the map representation. The map is more concrete in showing directly the charge density on a plane through the unit cell. Chosen proper planes one gets an immediate picture about the distribution of electrons in various regions. A map is, however, interesting only on a qualitative basis. Many planes are needed to cover the whole unit cell, and from a set of several maps it is not easy to create a clear view about the three-dimensional distribution. The view obtained of the distribution even on a single plane depends on the contour values used. and it is only through considerable experience one can learn to read and to interpret the maps, to discover essential features and to distinguish information from artefacts and noise. Even dramatic changes of single contour shapes may occur as a result of completely insignificant changes of the density. On the other hand, significant features may be left unobserved by occasional improper choice of contour values.

While the map representation gives a picture of the unit cell in slices the multipole representation builds the view of the unit cell of three-dimensional pieces, each showing one atom or a symmetric molecule with its immediate surroundings. The representation

of each piece is slightly more abstract since it does not immediately relate density values to certain points of the unit cell. Reading and interpreting the radial density curves requires a good comprehension of the behaviour of the symmetrized spherical harmonics in order to get the three-dimensional mental picture.

On the other hand the representation is quantitative. Large changes of radial density curves indicate significant changes of the density distribution and any significant features are very unlikely to remain unobserved. The information is given in an analysed form, since different low-order multipoles are coupled to different kinds of physical parameters. Also most of the expected interesting observations concern the motions and bonding of atoms i.e. features which are well in the range of the multipole representation and are easily described by low-order multipole components.

Calculation of radial densities through Eq. (2) and plotting the corresponding curves is straightforward and easy. No big computers or sophisticated computational techniques are necessary. So the multipole representation would certainly deserve a much wider use than at present.

3. TWO EXAMPLES

To demonstrate the use of the multipole representation we present two simple examples showing the different steps needed for formation and interpretation of the radial densities and comparing the representation with the use of the contour maps. We discuss the charge densities of the Cl^- ion in NaCl and of the OH^- ion in LiOH as they appear on the basis of the data by Göttlicher⁵ and Göttlicher and Kieselbach,⁶ respectively. The basic information required is listed in Table 1. In addition to what is needed for calculation of the conventional Fourier series the following basic data must be stated or defined for calculation of the multipole expansion:

1. The center of the expansion \mathbf{r}_0 . This is the position of the atom or molecule we wish to study, in this case the atomic site of chlorine in NaCl and that of oxygen in LiOH.
2. The site symmetry of the center. In addition to the point group ($m\bar{3}m$ and $4mm$) one has to state the orientation of the symmetry elements with respect to the crystal axes. It may also be useful to pay attention to possible approximate site symmetry as apparent from the co-ordination of the nearest neighbours.
3. The local co-ordinate system. This defines the meaning of the angular variables (θ, φ) and the explicit expressions of the symmetrized harmonics. When adapting the axes properly to the symmetry elements of the site. these are either real spherical

Table 1. Basic data for multipole analysis of NaCl and LiOH

	NaCl	LiOH
Space group	No. 225 Fm3m	No. 129 P4/nmm
Cell parameters	a=b=c=5.64056 Å $\alpha=\beta=\gamma=90^\circ$	a=b=3.549 Å c=4.334 Å $\alpha=\beta=\gamma=90^\circ$
Atomic positions	Na: 0,0, $\frac{1}{2}$ Cl: 0,0,0	Li: $\frac{1}{4},\frac{3}{4},0$ O : $\frac{3}{4},\frac{3}{4},0.194$ H : $\frac{3}{4},\frac{3}{4},0.407$
Experimental structure factors	S. Göttlicher ⁵	S. Göttlicher and B. Kieselbach ⁶
Maximum $\sin\theta/\lambda$	1.0029 Å ⁻¹	0.9976 Å ⁻¹
Theoretical model	Na ⁺ Cl ⁻	Li ⁺ O ⁻ (!)
Atomic factors	Int. Tables for X-ray Cryst. IV ²⁰	Int. Tables for X-ray Cryst. IV ²⁰
Isotropic temperature factors $\langle u^2 \rangle$	Na ⁺ : 0.02494 Å ² Cl ⁻ : 0.02119 Å ²	Li ⁺ : 0.02580 Å ² O ⁻ : 0.02190 Å ²
Site symmetry	Cl ⁻ : m3m	O ⁻ : 4mm
Matrix of local co-ordinate axes	$\begin{bmatrix} 1 & 0 & 0 \\ 0 & 1 & 0 \\ 0 & 0 & 1 \end{bmatrix}$	$\begin{bmatrix} 1 & 0 & 0 \\ 0 & 1 & 0 \\ 0 & 0 & 1 \end{bmatrix}$
Site-symmetrized harmonics, Kara and Kurki-Suonio ⁴	even octahedral (cubic $\ell=0,4,6,8,10,\dots$)	real spherical $y_{\ell mp}$ ($\ell,4\mu,+$)

harmonics or cubic harmonics with specific selection rules as indicated by Kara and Kurki-Suonio.⁴ In both of the present examples the natural local axes are just along the crystal axes i.e. have the directions $[100]$, $[010]$, $[001]$.

4. The multipole components to be calculated. Normally all components allowed by the symmetry up to some not very large order l should be calculated, cf. Kurki-Suonio.⁷ No definite rule can be given here for the maximum order. In discussion of approximate symmetries, it is informative to calculate also components allowed by the exact symmetry but not obeying the approximate symmetry because they indicate to which extent the charge density violates this symmetry.^{8,9}

The calculation of the radial densities (2) for any components is then straightforward. The expressions (1) and (2) are valid as such even when $Y_{\ell m p}$ are replaced by any spherical harmonics of a definite order l , e.g. cubic or icosahedral harmonics. This is useful to note in discussing the approximate symmetries where the harmonics orthogonal to the symmetric ones may have more complicated expressions in terms of $Y_{\ell m p}$.

Figures 1 and 2 show the radial difference densities for the low-order components in our examples. They refer to cubic harmonics $K_{\ell j}(\theta, \varphi)$ and real spherical harmonics $Y_{\ell m p}(\theta, \varphi)$, respectively, both normalized to maximum value 1, so that each curve shows directly the relevant contribution to the charge density in the direction (θ, φ) where it is largest. They were calculated using Eq. (2) as a

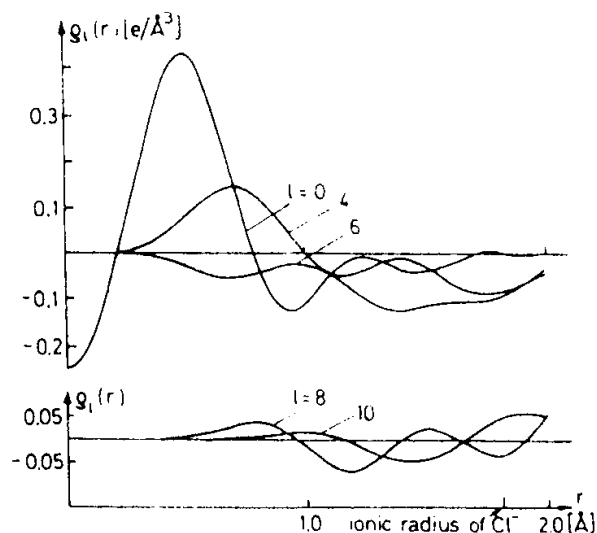


Fig. 1. Low-order radial difference densities of the site-symmetrized multipole expansion centered at the chlorine position in NaCl.

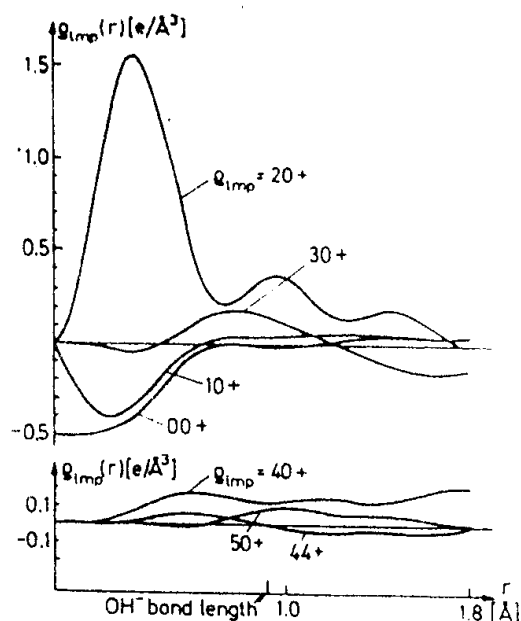
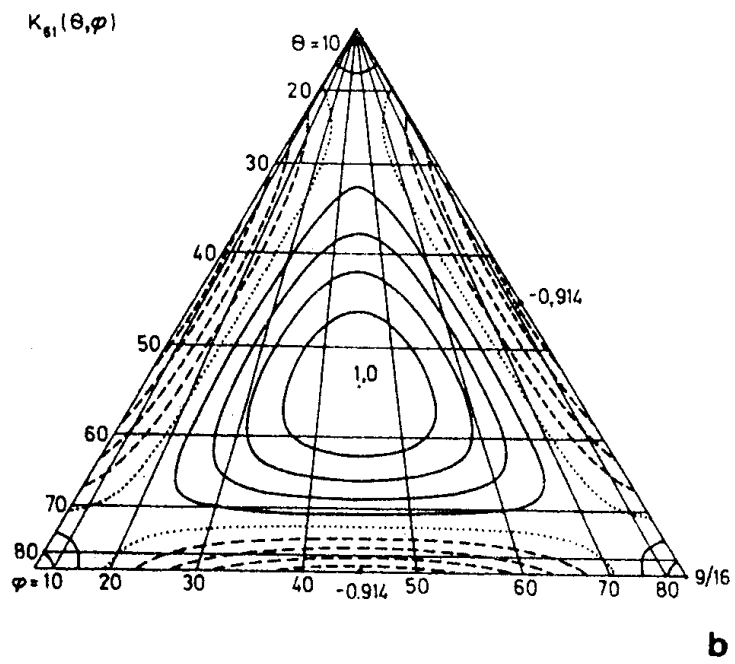
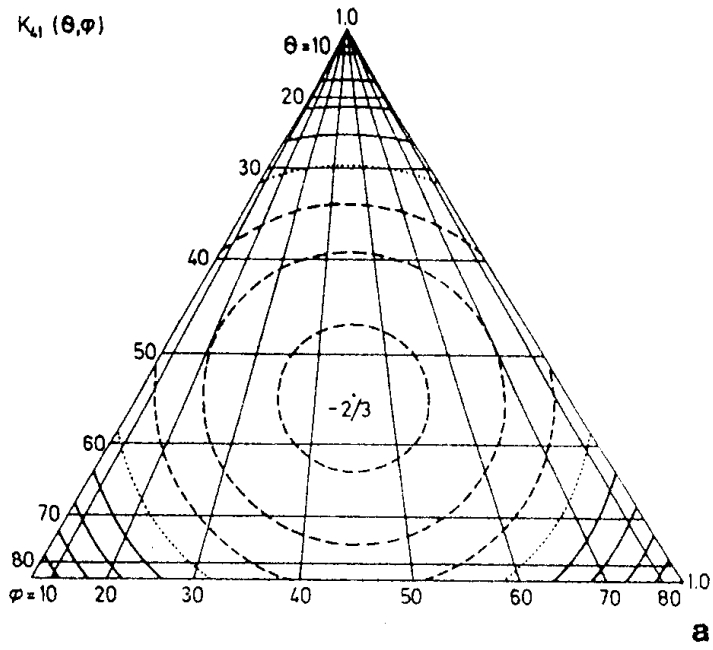


fig. 2. Low-order radial difference densities of the site-symmetrized multipole expansion centered at the oxygen position in LiOH.

difference series with coefficients $\Delta F = F_{\text{obs}} - F_{\text{theor}}$. In case of LiOR $\Delta F_{000} = 2$ must be included because there are two electrons missing from the model.

As far as the charge density of Cl^- or OH^- is concerned these are the results to be discussed. One has to learn to visualize these curves as a three-dimensional charge density. Each curve must be understood as multiplied by the corresponding harmonics to yield the three-dimensional contribution to the charge density. Therefore one needs a good acquaintance with the behaviour of low-order Legendre polynomials and associate Legendre functions which define the θ dependence of y_{imp} , as well as of the basic symmetry properties of the harmonics. Figures 3 a,b,c show the behaviour of the cubic harmonics K_4 , K_6 and K_8 , respectively, corresponding to the radial densities of Cl^- in Figure 1. The figure shows one octant of the surface of the unit sphere mapped on an equilateral triangle based on the correspondence $x^2=a$, $y^2=b$, $z^2=c$ where a,b,c are the distances of a point measured from the sides of the triangle. For a good mental picture it is sufficient to note the directions of the main maxima and minima.

So, for instance, we can read from Figure 1 the nature of the



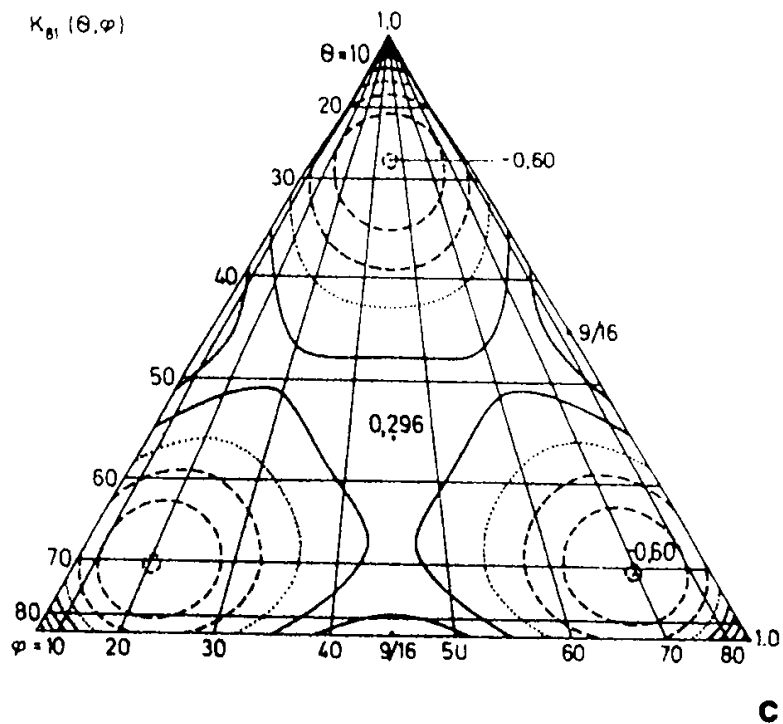


Fig. 3 a,b,c. Contour maps of the cubic harmonics $K_4(\theta, \varphi)$, $K_6(\theta, \varphi)$, $K_8(\theta, \varphi)$, respectively, normalized to $\text{Max}\{K_l\} = 1$ in the first octant. Contour interval 0.2, solid line positive, dashed line negative and dotted line zero.

deformations of chlorine as indicated by the data. The spherical component ρ_0 indicates a slight compression of the ion. In the core region, $r < 1 \text{ \AA}$, ρ_4 shows some transfer of charge from the [111] directions to the [100] directions. In the outer region, $r > 1 \dots 2 \text{ \AA}$, which from the point of view of bonding effects ought to be more interesting, the contributions to the density seem to be rather small. The nature of the 4th and 6th order deformations is, however, clear. Both reduce the density in the directions [100], thus effectively decreasing the overlap of the Cl^- and Na^+ as compared to the spherical ion model. They have partly cancelling effects in the [111] directions while the 6th order dominates in the [110] directions allowing an expansion of the chlorine towards the neighbouring chlorines.

Correspondingly, in Figure 2 ρ_{10+} indicates asymmetry of the charge distribution in the tetragonal axis direction. ρ_{20+} shows a symmetric elongation of the charge distribution along the tetragonal axis. The features at small r dominate the behaviour of both of these components, while all contributions look small at larger distances, which should be more interesting from the point of view of the effect of the hydrogen. (Note that there is no hydrogen included in F_{theor} .) At about the hydrogen distance it will be necessary to pay attention also to the main features of both $30+$ and $40+$. They are similar to those of $10+$ and $20+$ as described but concentrate to a narrower angular range around the tetragonal axis.

The correspondence between the radial densities and the conventional map representations is demonstrated in Figures 4a and 4b. They show the development of the multipolar charge density of the chlorine ion on the lines [100] and [111], respectively, with increasing number of multipoles as compared to the charge density calculated by Fourier series. The set of Figures 5 a,b,c,d show the corresponding development of multipolar charge density map on the plane $x=y$ through the chlorine as compared to the Fourier map. Similarly Figures 6 and 7 a,b,c,d show the development of multipolar charge density of the oxygen ion in LiOH along the z -axis and on the plane $x=0$ as compared to the corresponding Fourier representations.

Once the three-dimensional main features have been stated from the radial densities (Figures 1,2), their effect is clearly seen in the corresponding charge densities (Figures 4-7). It is, however, not quite clear how easily one could conclude backwards from the one- and two-dimensional representations, what are the main features three-dimensionally. Also, the shaping of the contour lines in the core region dominates the visual picture, while at the interesting distance $r = 1 \dots 2 \text{ \AA}$ it is much more difficult to deduce the essential features of the three-dimensional behaviour. For this purpose the multipole representation gives the information in a much more complete and concise form.

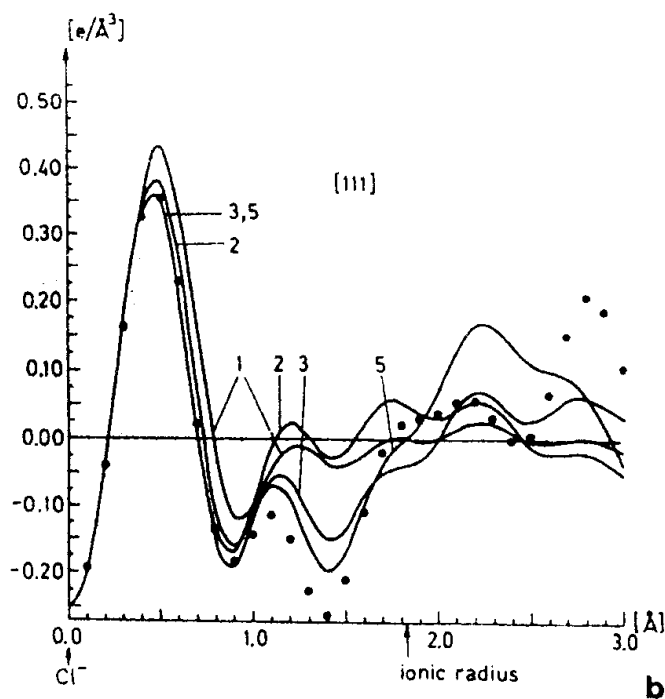
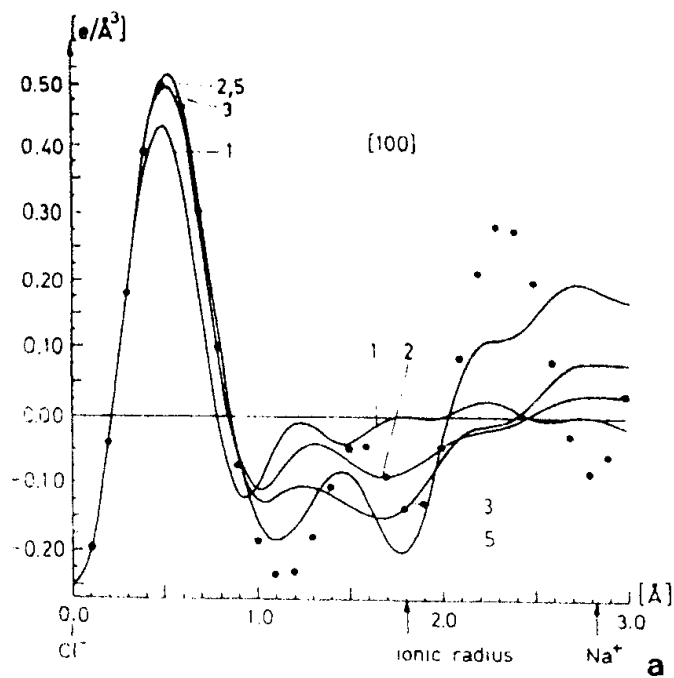
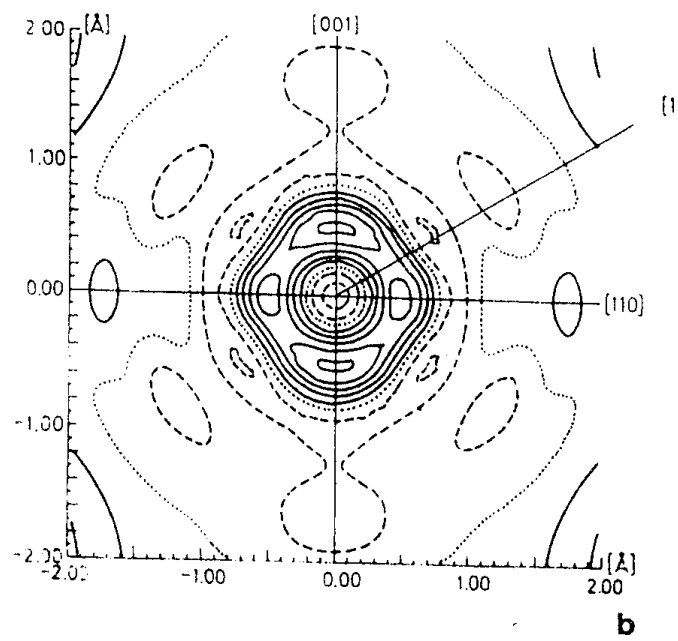
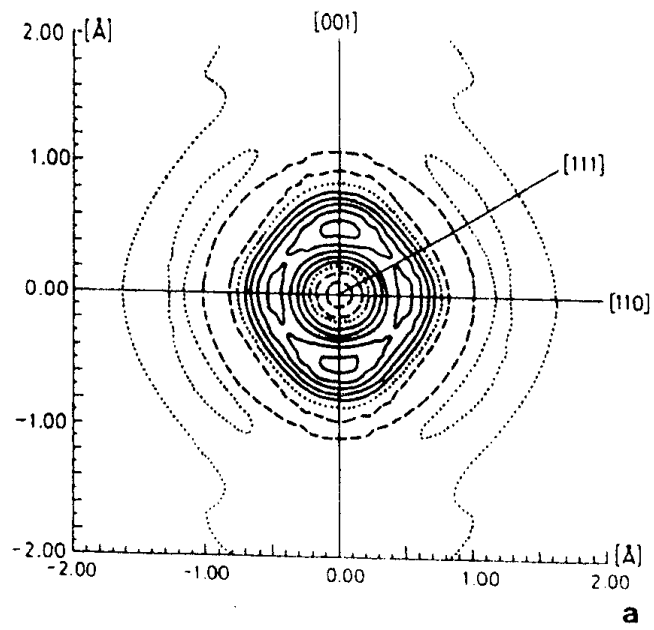


Fig. 4 a,b. Truncated multipole expansions of the difference charge density at the chlorine position in NaCl along the lines a) [100] and b) [111], as compared to the difference Fourier series (\bullet). The number of terms 1,2,3,5 as indicated in the figures corresponds to the maximum order $\ell = 0,4,6,10$, respectively.



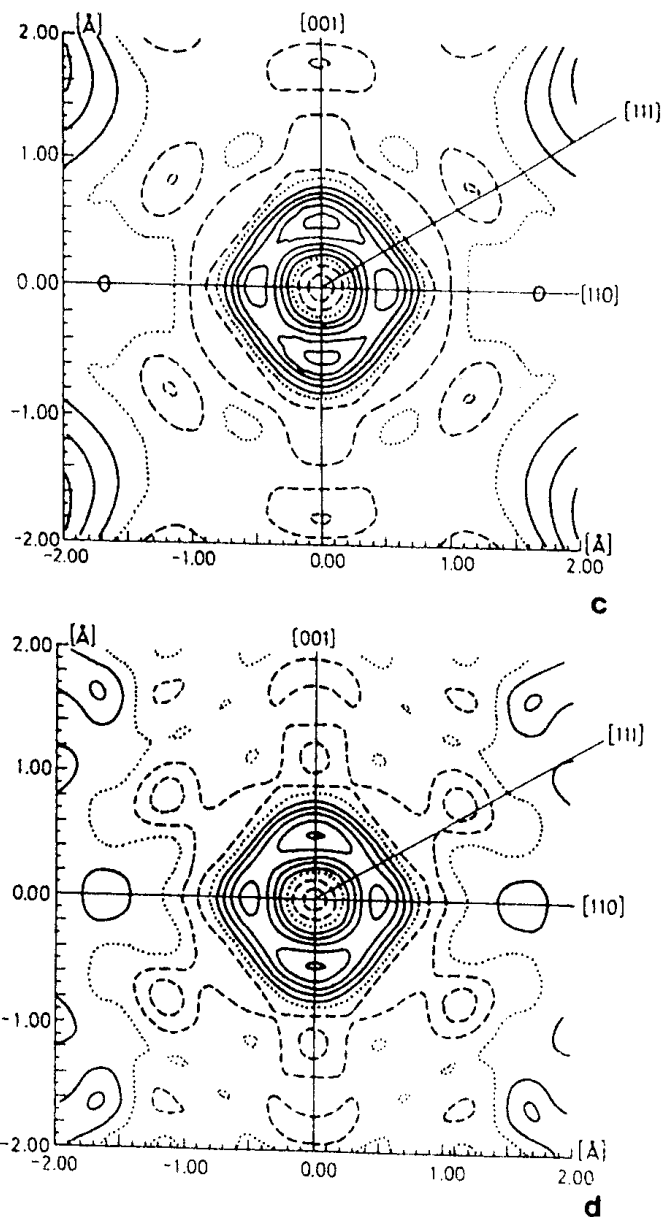


Fig. 5 a,b,c,d. Truncated multipole expansions of the difference charge density at the chlorine position in NaCl on the plane $x = y$ up to a) the 4th, b) the 6th and c) the 10th order as compared to d) the difference Fourier series. Contour interval $0.1 \text{ e}/\text{Å}^3$.

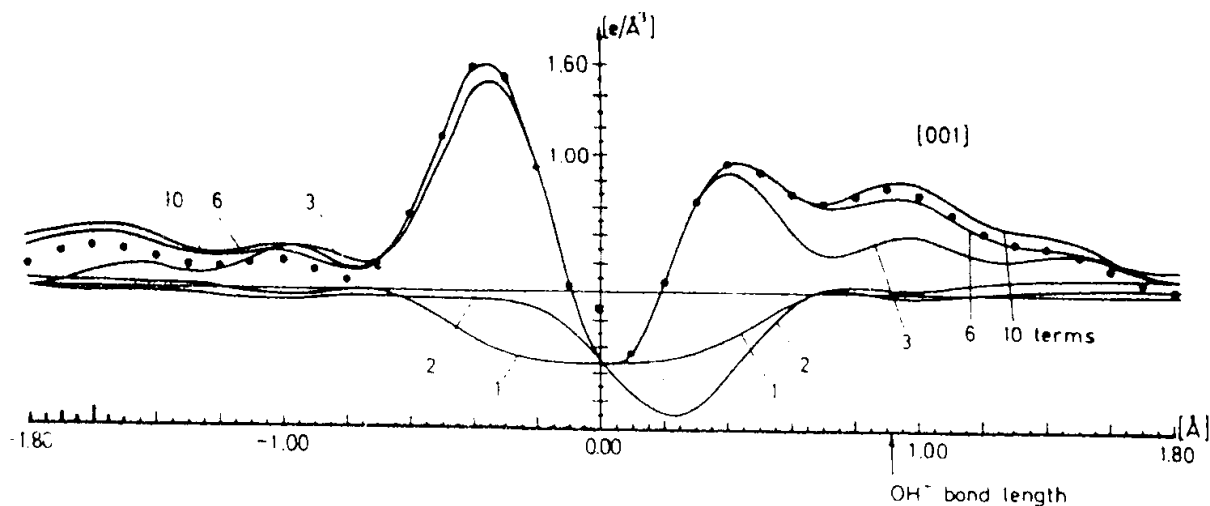


Fig. 6. Truncated multipole expansions of the difference charge density at the oxygen position in LiOH along the tetragonal axis as compared to the difference Fourier series. The number of terms 1, 2, 3, 6, 10 as indicated in the figure corresponds to the maximum order $\ell = 0, 1, 2, 4, 6$, respectively.

The only question then remains, how far we can rely upon having all important features included in the low order multipoles. To some extent this can be judged on the basis of convergence of the multipole expansion. The nature of the convergence is clearly visible in the Figures 4-7. We see that the convergence is very rapid in the main part of the atom up to about 1 Å distance from the center. In Cl^- three terms (up to the 6th order) and in OH^- three terms (up to the 2nd order) are sufficient to reproduce the shape of the ion. At larger distances higher orders get more important and, as is obvious, close to the distance of the nearest neighbour many more multipoles would be needed for reproduction of the Fourier series value of the density.

In the intermediate region, which is important in discussing the nature of bonding, a few more multipoles seem to give some contribution, and there still remain some deviations from the Fourier value. It is then important to be able to estimate the significance of these less smooth contributions and differences. On general physical arguments one would not expect to have strong high order components in the bonding region. Their presence is rather an indication of inaccuracies of the data. This is certainly true for any very local deviations.

One should remember that charge density is not a very favourable quantity to judge experimental significance of different

features because of the reciprocity of the representation space to the space of the experimental data. It is the number of electrons contributing in a feature which determines its significance rather than value of the charge density.^{7,10} From this point of view, the radial densities at some distance from the center express more reliably the significant feature. than charge density value. on any single line do, because they present an integrated behaviour over a whole spherical surface. There are, thus, good reasons to think that the smoothing of the Fourier series when presented by a low order multipole expansion is not a defect but an improvement of the picture, filtering away some unnecessary insignificant ripples.

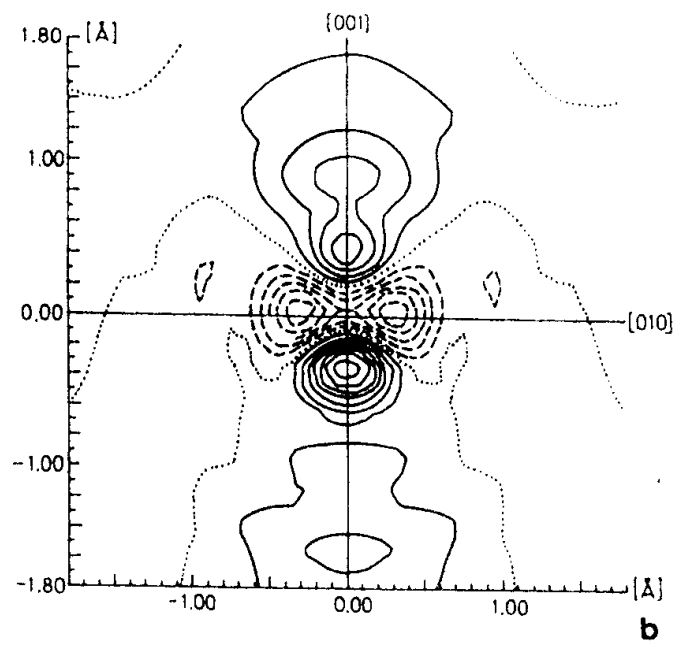
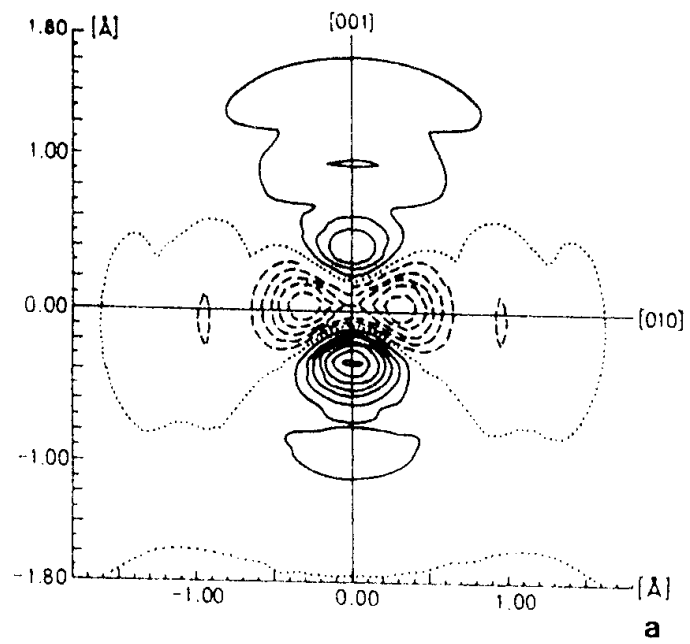
This brings us already close to the question about the ordinary purpose of the charge density representation. If the question is only about getting a clear qualitative over-all picture, then we can hardly convince anyone used to the maps to change over to multipoles. But as soon as we come to the quantitative analysis and interpretation of the data on basis of the representation, then the multipole expansion has some undeniable advantages over the maps.

4. QUESTIONS OF INTERPRETATION

An experienced track-finder is able to recognize also the origin of various features of his maps. He is able to see differences in position and in thermal parameters and many kinds of bonding effects. In the multi pole representation different effects are largely concentrated in different components and, thus, even more easily. recognizable:

Change of atomic position has a negligible effect on any other component than the first order. Moreover, the ratios of the three first order components express immediately the direction of the displacement, and the magnitude can be derived easily from their values at small r .

Difference in the harmonic temperature factor is visible in the zeroth and in the second order. Each of these six components indicates a difference of its own recognizable nature. The zeroth or monopole term refers to the average isotropic temperature parameter $\langle u^2 \rangle = (\langle u_x^2 \rangle + \langle u_y^2 \rangle + \langle u_z^2 \rangle) / 3$. Significant second order terms indicate anisotropy of the thermal motion. Assuming the local xyz-co-ordinate system to coincide with the thermal axes, 20+ indicates a difference in prolateness or $\langle u_z^2 \rangle - \langle u^2 \rangle$, 22+ implies necessity to correct the non-axiality or $\langle u_x^2 \rangle - \langle u_y^2 \rangle$. Rotation of the anisotropic thermal ellipsoid about the local x-, y- and z-axes gives rise to the components 21-, 21+ and 22-, respectively. Each of these effects is visible only in the relevant component with negligible effect on the others.



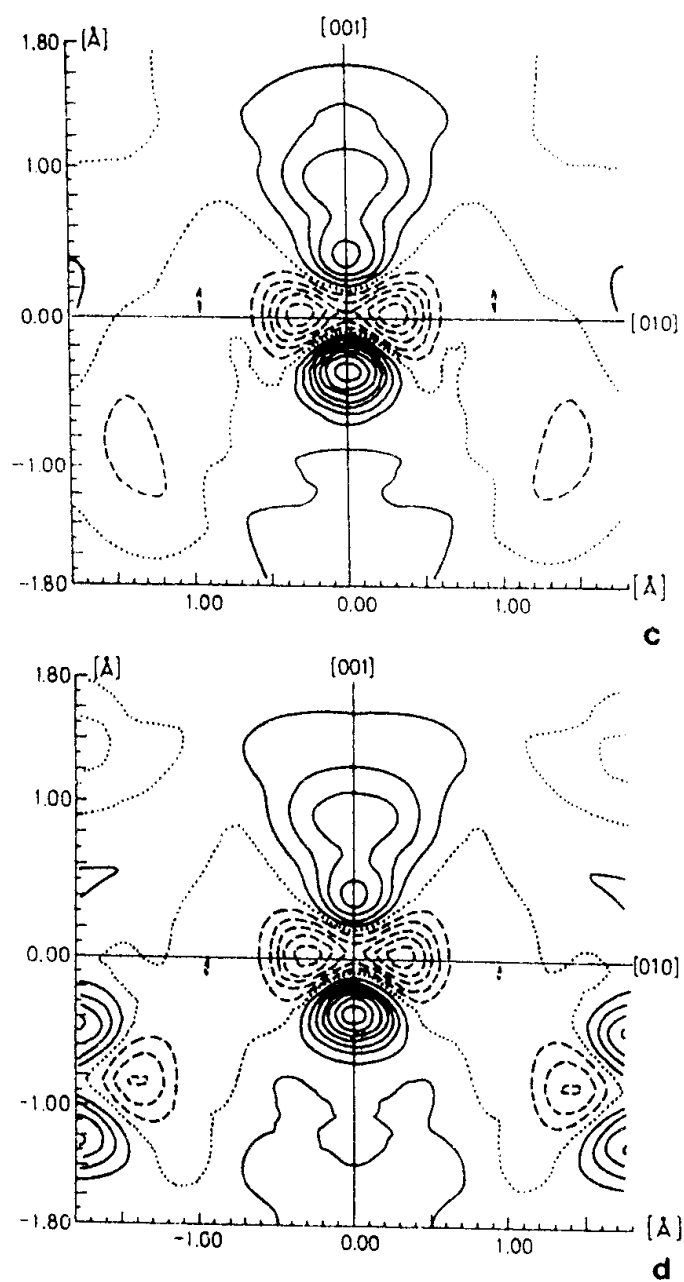


Fig. 7 a,b,c,d. Truncated multipole expansions of the difference charge density at the oxygen position in LiOH on the plane $x = 0$ up to a) the 2nd, b) the 4th, c) the 6th order as compared to d) the difference Fourier series. Contour interval $0.2 e/\text{Å}^3$.

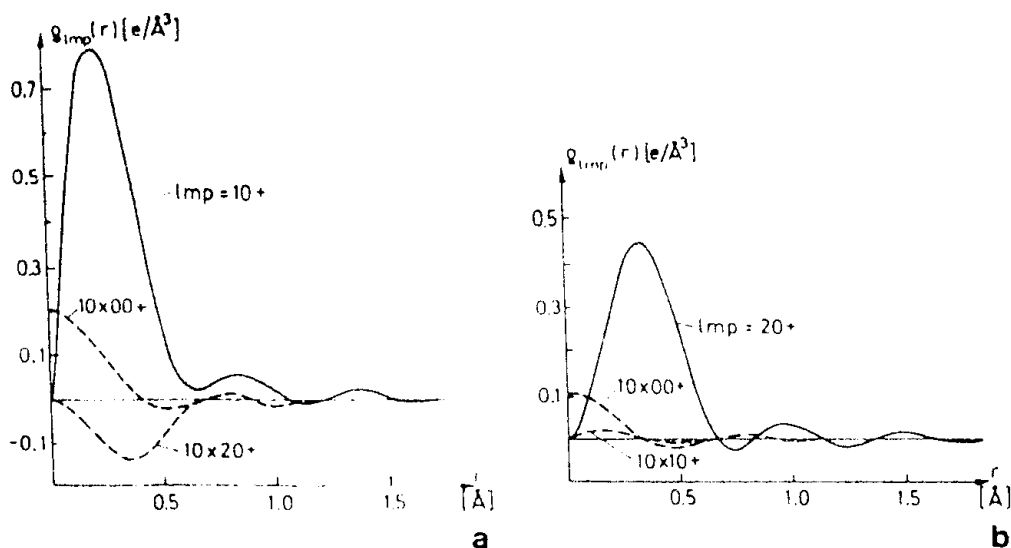


Fig. 8 a,b. The effect of
 a) the change $\Delta z = 0.01 \text{ \AA}$ of the oxygen position
 b) introducing prolateness $\langle u_z^2 \rangle - \langle u^2 \rangle = 0.002 \text{ \AA}^2$
 of the thermal motion of oxygen
 on the radial densities centered at the oxygen in LiOH.

To demonstrate this good separation of information we show in the Figures 8a and 8b the radial densities caused by a change $\Delta z = 0.01 \text{ \AA}$ in the position of the oxygen in LiOH and by introducing a prolateness $\langle u_z^2 \rangle - \langle u^2 \rangle = 0.002 \text{ \AA}^2$ to its thermal motion, respectively. Both figures are results of a pure model calculation involving no experimental data. They show very clearly that conclusions on the position and on the anisotropy must be based merely on the components 10+ and 20+, respectively. At the same time we recognize that the component 20+ in Figure 2 is mostly due to anisotropy of the thermal motion. Comparison of the magnitudes would give the value 0.0070 \AA for the prolateness parameter of the oxygen. Similarly we can conclude that moving the oxygen from the position $z = 0.8408 \text{ \AA}$ by 0.0052 \AA down the z-axis would make ρ_{10+} vanish without effecting any other components.

Reading quantitative information on other effects, say features which qualitatively are described as electronic deformations or bonding effects is also possible although less straightforward. There are better means than the radial densities themselves to judge the significance of such features, viz. calculation of radial scattering factors corresponding to the different multipoles by spherical volume partition techniques.⁷ Also the functions $4\pi r^2 \rho_{lmp}(r)$ show the significance of different features more clearly, since the area under the curve is directly related to the number of electrons contributing

to the deformation described by the component. Quantitative conclusions require then knowledge about the integrals of the harmonics over their lobes. For instance, knowing that the integral of K_4 over its positive lobes is 2.30 we can conclude from ρ_4 in Figure 1 that the angular transfer of electrons involved in the "core deformation" ($r < 1 \text{ \AA}$) is only 0.07, which is at the limit of significance. The corresponding number in the region $r = 1 \dots 2 \text{ \AA}$ is 0.3 electrons, which is significant.

In our second example the effect of the hydrogen atom is seen as an electronic deformation of the oxygen. We already saw that visually dominant features can be explained just as small non-interesting corrections to conventional parameters. To discuss the deformation we have to look at the features which at the first sight seem to be small and in fact are small in terms of local density values. However, redrawing the components as $4\pi r^2 \rho_{\ell mp}(r)$ would reveal the real relative significance of different features as integrated large-scale features. Taking into account the integrals of $Y_{\ell 0}$ over their main positive lobes we find that the $10+$ -asymmetry of OH^- , which extends rather far from the center, involves the total of only about 0.3 electrons, while the symmetric $20+$ deformation, beyond the anisotropy effect, is much larger involving about 0.75 electrons. The $30+$ does not add to the integral value of charge asymmetry, but it pushes the excess charge closer to about the hydrogen distance. Also, the $40+$ does not essentially add to the charge of the symmetric deformation. It makes it to concentrate to a narrower angular region around the z-axis.

5. SUMMARY

Multipole expansions in the sense they have been discussed in this paper have been applied on both neutron and X-ray data. They have been seen to be most advantageous in case of simple inorganic structures. While providing a simple means of representing the charge density they give an immediate three-dimensional picture and, at the same time, show the information in a well-analyzed form. Different components indicating different kinds of effects. Moreover, it is easy to proceed from it into quantitative determination of physically and chemically meaningful parameters. One has been able to see bonding effects, spherical and aspherical deformations of ions,⁸⁻¹⁵ anharmonicities of motions,^{9,16} librations and preferred orientations of small rigid molecules.¹⁷⁻¹⁹

The easy adaptation of multipole expansions to any symmetries makes them valuable in studying possible approximate symmetries or deviations from them.^{8,9} On the other hand the number of applications is still rather small. So far almost every single application has revealed some interesting new possibilities or problems. A recent study of BeO has proved that even the phase problem of non-centric

crystals can be properly treated.⁹ It seems that as a means of analysis the multipole expansion would be most profitable when used beside the conventional least squares method to guide the refinement process. As a representation it may similarly find its best use as a simple complementary method to show quantitatively some interesting three-dimensional features, which can be seen from the charge density maps only incompletely and qualitatively.

REFERENCES

1. V.H. Smith, Jr., P.F. Price, and I. Absar, *Isr. J. Chem.* 16, 187-197 (1977).
2. M. Atoji, *Acta Cryst.* 11, 827-829 (1958).
3. K. Kurki-Suonio, *Isr. J. Chem.* 16, 115-123 (1977).
4. M. Kara and K. Kurki-Suonio, *Acta Cryst. A* 37, 201-210 (1981).
5. S. Göttlicher, *Acta Cryst. B* 24, 122-129 (1968).
6. S. Göttlicher and B. Kieselbach, *Acta Cryst. A* 32, 185-192 (1976).
7. K. Kurki-Suonio, *Acta Cryst. A* 24, 379-390 (1968).
8. J.P. Vidal, G. Vidal-Valat, M. Galtier, and K. Kurki-Suonio, *Acta Cryst. A* 37, 826-837 (1981).
9. J.P. Vidal, G. Vidal-Valat, M. Galtier, and K. Kurki-Suonio, (to be published).
10. K. Kurki-Suonio, Italian Crystallographic Association Meeting, Bari, Italy, 1971. Congress Report 31-66 (1972).
11. K. Kurki-Suonio and A. Ruuskanen, *Ann. Acad. Sci. Fenn. Ser. A VI* 358, 1-29 (1971).
12. K. Kurki-Suonio and V. Meisalo, *Ann. Acad. Sci. Fenn. Ser. A VI* 241, 1-18 (1967).
13. M. Linkoaho, E. Rantavuori, U. Korhonen, K. Kurki-Suonio, and A. Ruuskanen, *Acta Cryst. A* 28, 260-264 (1972).
14. A. Ruuskanen and K. Kurki-Suonio *J. Phys. Soc. Japan* 34, 715-719 (1973).
15. G. Vidal-Valat, J.P. Vidal, and K. Kurki-Suonio, *Acta Cryst. A* 34, 594-602 (1978).
16. M. Ahtee, K. Kurki-Suonio, A. Vahvaselkä, A.W. Hewat, J. Harada, and S. Hirotsu, *Acta Cryst. B* 36, 1023-1028 (1980).
17. K. Kurki-Suonio, M. Merisalo, A. Vahvaselkä, and F.K. Larsen *Acta Cryst. A* 32, 110-115 (1976).
18. A. Vahvaselkä and K. Kurki-Suonio, *Physica Fennica* 10, 87-99 (1975).
19. M. Ahtee, K. Kurki-Suonio, B.W. Lucas, and A.W. Hewat, *Acta Cryst. A* 35, 591-597 (1979).
20. *International-Tables for X-ray Crystallography*, vol. IV, The Kynoch Press, Birmingham, 1974.